Modeling distributed axonal delays in mean-field brain dynamics

J. A. Roberts[1,2,*] and P. A. Robinson[1,2,3]
[1]*School of Physics, University of Sydney, New South Wales 2006, Australia*
[2]*Brain Dynamics Centre, Westmead Millenium Institute, Westmead Hospital and Western Clinical School of The University of Sydney, Westmead, New South Wales 2145, Australia*
[3]*Faculty of Medicine, University of Sydney, New South Wales 2006, Australia*
(Received 18 June 2008; revised manuscript received 2 September 2008; published 3 November 2008)

The range of conduction delays between connected neuronal populations is often modeled as a single discrete delay, assumed to be an effective value averaging over all fiber velocities. This paper shows the effects of distributed delays on signal propagation. A distribution acts as a linear filter, imposing an upper frequency cutoff that is inversely proportional to the delay width. Distributed thalamocortical and corticothalamic delays are incorporated into a physiologically based mean-field model of the cortex and thalamus to illustrate their effects on the electroencephalogram (EEG). The power spectrum is acutely sensitive to the width of the thalamocortical delay distribution, and more so than the corticothalamic distribution, because all input signals must travel along the thalamocortical pathway. This imposes a cutoff frequency above which the spectrum is overly damped. The positions of spectral peaks in the resting EEG depend primarily on the distribution mean, with only weak dependences on distribution width. Increasing distribution width increases the stability of fixed point solutions. A single discrete delay successfully approximates a distribution for frequencies below a cutoff that is inversely proportional to the delay width, provided that other model parameters are moderately adjusted. A pair of discrete delays together having the same mean, variance, and skewness as the distribution approximates the distribution over the same frequency range without needing parameter adjustment. Delay distributions with large fractional widths are well approximated by low-order differential equations.

DOI: 10.1103/PhysRevE.78.051901 PACS number(s): 87.19.L−, 87.10.−e, 02.30.Ks

I. INTRODUCTION

Transmission delays are inherent in physical systems and responsible for rich dynamics. In many neural systems, these delays are of key importance and cannot be neglected in modeling. Axonal delays in the brain can be grouped into two categories: delays within a given structure (such as within the cortex) and delays between distinct structures (such as between cortex and thalamus). While numerous studies have explored the properties of delays within a single structure [1–10], less attention has been devoted to the delays between structures [9–13], which until now have only been treated in detail by approximating them as single discrete delays. In this paper we relax this restriction, and explore the effects of temporally distributed delays between cortex and thalamus in a physiologically based mean-field model [8–16]. We concentrate on the temporal aspects of these delays, so as not to obscure their effects with other effects due to spatial propagation. For similar reasons, we also assume a translation-invariant form for intracortical delays, and focus on the linear regime with spatially uniform parameters; nonlinear effects and spatial inhomogeneities are straightforward to include, in the same ways as in previous work [1,2,4–6,8–12,15].

Delays both within and between populations have been modeled as convolutions over the history of the source activity [5,6,10], taking into account the spatiotemporal distribution of delays, although for many applications such an integral representation is both analytically and numerically undesirable. Certain connection topologies enable useful simplifications. For example, propagation within neuronal populations has been shown to obey a damped wave equation to a good approximation [1,2,4,8,9], yielding a convenient differential form in both space and time. In neural networks, the mean activity can be described by a purely temporal convolution [3,7]. The spatial convolution can also be neglected between structures connected by a one-to-one spatial mapping, such as occurs between cortex and thalamus [9–11,13]. This includes the case in which the delay is approximately independent of position, as has recently been shown in the mouse thalamocortical pathway [17].

One common simplification to a temporal distribution of delays is to induce an effective delay via the phase shift of a simple low-pass filter, which yields ordinary differential equations (ODEs) for appropriate choices of filter. Another useful simplification is to replace the delay distribution with a single discrete delay, resulting in a delay differential equation (DDE). The conditions under which a distribution of delays with nonzero width is suitably approximated by a single discrete delay are yet to be determined. Care must be taken in general, because the introduction of discrete delays can destabilize the system [7,18]. As discrete delays are commonly used in the literature [9–13,15,19,20], this is an important point to resolve. We address this issue in the context of a mean-field corticothalamic model of neuronal activity.

The EEG is a commonly used diagnostic of brain function, exhibiting spectral peaks at ~10 Hz (termed alpha) and ~20 Hz (termed beta) during healthy resting states [1,4]. There is significant evidence that the positions of these peaks are determined primarily by the thalamocortical and corticothalamic delays [9,11–13]. How the generation of these peaks is related to the distribution of physiological delays is

*jamesr@physics.usyd.edu.au

unknown, and is also relevant to deciding the validity of such mechanisms, but comparison of the various competing models for this phenomenon is beyond the scope of this paper. Additionally, the distribution of human delays is itself only indirectly inferred, with the only estimates obtained by extrapolation from other mammals such as the cat. The dynamics of the corticothalamic system constrain the allowable delay distributions.

The paper is organized as follows. In Sec. II, we model distributed delays between distinct neural populations, and incorporate them into a mean-field model of brain dynamics [8–16]. In Sec. III, we explore the implications of allowing a range of thalamocortical and corticothalamic delays on the EEG spectrum, giving conditions for discrete delays and ODEs to yield reasonable approximations of delay distributions.

II. THEORY

In this section, we model distributed delays between distinct neural populations and incorporate them into the model of Robinson *et al.* [8–16]. Section II A shows how distributed delays linearly filter an input signal, while in Sec. II B we derive the white-noise driven linear power spectrum for general distributed thalamocortical and corticothalamic delays, the effects of which we will show in Sec. III.

A. Distributed delays

In previous work, the transmission delay between two neuronal populations was modeled as a single discrete delay in the form $\phi_b(t-\tau_{ab})$, for input to population a from population b with delay τ_{ab} [9–16]. Here we generalize the delayed transmission to take into account a distribution of delay times [10]. We focus on delays *between* populations, rather than the spatiotemporal delays *within* a single population [5,6,10], in order to treat these delays separately. The input $\psi_{ab}(t)$ to population a is now a convolution over the history of population b, given by

$$\psi_{ab}(t) = \int_{-\infty}^{\infty} M_{ab}(t-t')\phi_b(t')dt', \tag{1}$$

where $M_{ab}(t)$ is the normalized distribution of delay times, and $M_{ab}(t)=0$ for $t<0$ ensures that the input is causal. Instantaneous connections (i.e., $\tau_{ab}=0$) have $M_{ab}(t-t')=\delta(t-t')$, and the discrete delay case is recovered for $M_{ab}(t-t')=\delta(t-t'-\tau_{ab})$.

Equation (1) linearly filters input $\phi_b(t)$ producing output $\psi_{ab}(t)$. Rather than evaluate the integral in Eq. (1), we use the filter's transfer function, enabling efficient calculation of the response to a variety of inputs. This is ideally suited to linear analysis of any model containing Eq. (1), enabling derivation of the noise-driven linear power spectrum and stimulus-evoked responses, which are of key interest in electroencephalography. Fourier transforming Eq. (1) gives the transfer function

$$M_{ab}(\omega) = \frac{\psi_{ab}(\omega)}{\phi_b(\omega)}, \tag{2}$$

where $M_{ab}(\omega)$, $\psi_{ab}(\omega)$, and $\phi_b(\omega)$ are the Fourier transforms of $M_{ab}(t)$, $\psi_{ab}(t)$, and $\phi_b(t)$, respectively.

Certain choices of $M_{ab}(t)$ such that $M(\omega)=R(i\omega)$, where $R(i\omega)$ is a rational function of $i\omega$, allow us to express Eq. (1) in a linear differential form. For example, if $M_{ab}(\omega)=1/p(i\omega)$, where $p(i\omega)$ is a polynomial in $i\omega$ of order n, then a linear differential operator $T_{ab}(t)=\mathcal{F}^{-1}\{p(i\omega)\}$ exists and is also of order n, such that

$$T_{ab}\psi_{ab}(t) = \phi_b(t). \tag{3}$$

One distribution with this property is the gamma distribution,

$$M_{ab}(t) = \frac{\mu^n}{\Gamma(n)}t^{n-1}e^{-\mu t}H(t), \tag{4}$$

where n, $\mu>0$ are real parameters, and $H(t)$ is the unit step function. This distribution has mean $\langle t\rangle=n/\mu$, mode $t_{\mathrm{pk}}=(n-1)/\mu$, standard deviation $\Delta t=\sqrt{n}/\mu$ (which we take to be the characteristic width), and Fourier transform $M_{ab}(\omega)=(1-i\omega/\mu)^{-n}$. Thus $M_{ab}(\omega)$ is of the form $1/p(i\omega)$ when n is an integer, and Eq. (3) becomes

$$\left(1+\frac{1}{\mu}\frac{d}{dt}\right)^n \psi_{ab}(t) = \phi_b(t). \tag{5}$$

Note that by setting $n=(\tau_{ab}/\sigma_{ab})^2$ and $\mu=\tau_{ab}/\sigma_{ab}^2$ in Eq. (4), we can parametrize the gamma distribution by its mean $\langle t\rangle=\tau_{ab}$ and standard deviation $\Delta t=\sigma_{ab}$. With τ_{ab} fixed, in the limit $\sigma_{ab}\to 0$ we have $M_{ab}(\omega)\to e^{i\omega\tau_{ab}}$ and $\psi_{ab}(t)\to\phi_b(t-\tau_{ab})$, recovering the discrete delay case again.

An example of a distribution for which we can calculate the transfer function analytically, but which does not permit an equivalent differential equation representation, is the Gaussian distribution truncated at $t=0$. It has probability density function

$$M_{ab}(t) = \frac{1}{\sigma\sqrt{2\pi}A_0}\exp\left[-\frac{(t-\tau)^2}{2\sigma^2}\right]H(t), \tag{6}$$

where τ, $\sigma>0$ are parameters, and $1/2<A_0=[1+\mathrm{erf}(\tau/\sigma\sqrt{2})]/2<1$ is a factor correcting for the truncation; the normalization factor for the full Gaussian is recovered when $A_0\to 1$. This distribution has mean

$$\langle t\rangle = \tau + \frac{\sigma}{A_0\sqrt{2\pi}}\exp\left(-\frac{\tau^2}{2\sigma^2}\right), \tag{7}$$

standard deviation Δt given by

$$(\Delta t)^2 = \sigma^2 - \frac{\sigma}{A_0\sqrt{2\pi}}\exp\left(-\frac{\tau^2}{2\sigma^2}\right)\langle t\rangle, \tag{8}$$

and Fourier transform

$$M_{ab}(\omega) = \frac{1}{2A_0} \exp\left(i\omega\tau - \frac{\sigma^2\omega^2}{2} \right) \left[1 + \mathrm{erf}\left(\frac{\tau + i\omega\sigma^2}{\sigma\sqrt{2}} \right) \right]. \tag{9}$$

Note that while $M_{ab}(t)$ is discontinuous at the origin, $\lim_{t\to 0^+} M_{ab}(t)$ is small if $\sigma \ll \tau$, i.e., if the distribution is confined sufficiently far from the origin. In this limit the response is essentially the same as that of the full Gaussian. Thus $\langle t \rangle \approx \tau$, $\Delta t \approx \sigma$, and $M_{ab}(\omega) \approx \exp(i\omega\tau - \sigma^2\omega^2/2)$ for small ω [for large ω, $|M_{ab}(\omega)| \sim 1/\omega$ instead of $|M_{ab}(\omega)| \sim \exp(-\sigma^2\omega^2/2)$ for the full Gaussian]. Note that gamma- and Gaussian-distributed delays are commonly observed in mammalian brains [21,22].

It is important to determine when one or more discrete delays are a good approximation to a wide distribution of delays, because discrete delays are computationally easier to handle, unless an equivalent low-order ODE exists. For n discrete delays, the distribution is

$$M_{ab}(t) = \sum_{k=1}^{n} c_k \delta(t - \tau_k), \tag{10}$$

with Fourier transform

$$M_{ab}(\omega) = \sum_{k=1}^{n} c_k e^{i\omega\tau_k}, \tag{11}$$

where τ_k are the delays and c_k are positive constants satisfying $\Sigma_{k=1}^{n} c_k = 1$. For $n=2$, the distribution has mean $\langle t \rangle = c_1\tau_1 + c_2\tau_2$, and variance $(\Delta t)^2 = c_1c_2(\tau_1 - \tau_2)^2$.

The transfer function $M_{ab}(\omega)$ describes how propagation to a distorts the signal from b. Specifically, the magnitude $|M_{ab}(\omega)|$ is the frequency-dependent gain of the filter, the power output $|\psi_{ab}(\omega)|^2 = |M_{ab}(\omega)|^2 |\phi_b(\omega)|^2$ is proportional to the squared gain, and $\tau_g = d[\arg M_{ab}(\omega)]/d\omega$ is the frequency-dependent group delay. The case of a discrete delay τ_{ab} has $M_{ab} = e^{i\omega\tau_{ab}}$, so that any input signal passes through with amplitude unchanged and delay $\tau_g = \tau_{ab}$. A pair of equally weighted delays ($c_1 = c_2 = 1/2$) separated by $2\sigma = |\tau_2 - \tau_1|$ has $|M(\omega)| = |\cos(\omega\sigma)|$, so $M(\omega) = 0$ at $\omega = m\pi/2\sigma$ for m odd, where signals arriving at delays τ_1 and τ_2 are out of phase. These zeros constrain the range of frequencies that can propagate from b to a. Note that $M_{ab}(0) = 1$, and $|M_{ab}(\omega)|^2$ falls to $|M_{ab}(\omega_m)|^2 = 1/2$ at $\omega = \omega_m = \pi/4\sigma$, where ω_m is the frequency below which more than half of the power at each ω is transmitted. Thus undamped signal propagation in a contiguous band between $\omega = 0$ and high frequencies requires closely spaced delays. Setting unequal weights $c_1 \neq c_2$ for τ_1 and τ_2 gives $|M_{ab}(\omega)|^2 = 1 - 4c_1c_2 \sin^2(\omega\sigma)$, eliminating the zeros, but the gain is still minimized at these frequencies. If $c_1c_2 < 1/8$, $|M_{ab}(\omega)|^2 > 1/2$ for all ω.

For both the gamma and Gaussian distributions, $|M_{ab}(\omega)|^2$ decreases monotonically and tends to zero as $\omega \to \infty$, imposing a high-frequency cutoff. For gamma-distributed delays, $|M_{ab}(\omega)|^2 = (1 + \omega^2/\mu^2)^{-n}$, giving a cutoff $\omega_m = \sqrt{\ln 2}/\sigma$ when $\tau \gg \sigma$, and $\omega_m = 1/\sigma$ when $\tau \approx \sigma$. For Gaussian-distributed delays with $\tau \gg \sigma$, $|M_{ab}(\omega)|^2 \approx e^{-\omega^2\sigma^2}$, giving a cutoff $\omega_m = \sqrt{\ln 2}/\sigma$ as well. Thus the width of the delay distribution constrains the frequencies transmitted to satisfy $\omega \lesssim \omega_m = 1/\sigma$, implying that a narrow distribution is needed to pass high frequencies. The narrower the distribution is, the higher is the upper frequency bound below which signals will arrive in phase.

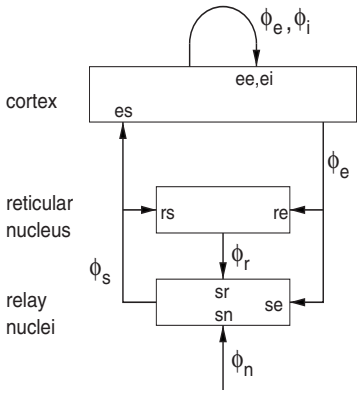

FIG. 1. Schematic connectivities between neuronal populations in the model. Cortical populations (excitatory $a=e$, inhibitory $a=i$) and thalamic populations (relay $a=s$, reticular $a=r$) are shown, with arrows labeled ab denoting where the fields ϕ_b project, with connection strength ν_{ab} for input to population a from population b (see text for details). Input from the brainstem enters the system in ϕ_n.

Note that $M_{ab}(\omega)$ is also the characteristic function of $M_{ab}(t)$ [23]. Expanding $M_{ab}(\omega)$ about $\omega = 0$ gives

$$M_{ab}(\omega) = \sum_{k=0}^{\infty} \frac{(i\omega)^k}{k!} \mu'_k, \tag{12}$$

where μ'_k is the kth moment of $M_{ab}(t)$, with $\mu'_0 = 1$. Thus the agreement at low frequencies between the dynamics resulting from two distributions improves with increasing number of moments equal between them. We use this fact in Sec. III.

B. Incorporating distributed delays into the corticothalamic model

Here we incorporate distributed delays into the specific corticothalamic model of Refs. [8–16], deriving the power spectrum for general thalamocortical and corticothalamic delay distributions. The model is outlined briefly here, full details having been presented elsewhere [8–11,13]. The neuronal populations modeled are the excitatory (e) and inhibitory (i) cortical neurons, and the specific relay (s) and reticular nucleus (r) of the thalamus, with external input from the brainstem and elsewhere (n) driving the system through s. A schematic of the system is shown in Fig. 1.

The delayed terms in the corticothalamic model appear only in the equations for the cell body potential V_a [8–11,13], which are now

$$V_a(\mathbf{r},t) = \sum_b V_{ab}(\mathbf{r},t), \tag{13}$$

$$D_{ab}(t) V_{ab}(\mathbf{r},t) = \nu_{ab} \psi_{ab}(\mathbf{r},t), \tag{14}$$

$$D_{ab}(t) = \frac{1}{\alpha_{ab}\beta_{ab}}\frac{d^2}{dt^2} + \left(\frac{1}{\alpha_{ab}} + \frac{1}{\beta_{ab}}\right)\frac{d}{dt} + 1, \qquad (15)$$

where we have replaced $\phi_b(\mathbf{r}, t-\tau_{ab})$ with $\psi_{ab}(\mathbf{r},t)$ given by Eq. (1) (with spatial dependence included). Subpotential $V_{ab}(\mathbf{r},t)$ is the contribution to the mean cell body potential of population a from neurons in population b. Connection strength $\nu_{ab}=N_{ab}s_{ab}$, where N_{ab} is the mean number of synapses on neurons of type a from neurons of type b, and s_{ab} is the strength of response to a unit input from neurons of type b. The differential operator $D_{ab}(t)$ models the synaptodendritic response of the cell body potential, where α_{ab} and β_{ab} are the inverse decay and rise times of the soma response to input b, respectively. For the model in Fig. 1, the only nonzero τ_{ab} are the thalamocortical delays $\tau_{es}=\tau_{is}$ and the corticothalamic delays $\tau_{se}=\tau_{re}$. We retain this connectivity here, with the only $M_{ab}(\omega)\neq 1$ being $M_{es}=M_{is}$ and $M_{se}=M_{re}$. Intracortical propagation obeys a damped wave equation to a good approximation [1,2,4,8–11,13], giving rise to distance-dependent delays within the cortex, as distinct from the propagation between structures that is our focus. Owing to the short range of cortical inhibitory axons, and the relative smallness of the thalamus, we neglect the wave propagation within these populations [9,11,13].

The power spectrum $P(\omega)$ can be calculated for any delay distribution $M_{ab}(t)$, without the delay kernel necessarily allowing a differential form. If $M_{ab}(\omega)$ can be obtained in closed form, then so too can $P(\omega)$, and in any case $P(\omega)$ can be obtained much more efficiently numerically via the transfer function than by solving the full system of differential equations. Using Eq. (2) and the other model equations (see Ref. [13] for details), we obtain $P(\omega)$ for fluctuations about a fixed point, yielding

$$P(\omega) = \frac{\langle\phi_n^2\rangle}{4\pi r_e^4}\left|\frac{G_{esn}L_{es}L_{sn}M_{es}}{(1-G_{ei}L_{ei})(1-G_{srs}L_{sr}L_{rs})}\right|^2\left|\frac{\mathrm{Arg}q^2}{\mathrm{Im}\,q^2}\right|, \qquad (16)$$

$$q^2r_e^2 = \left(1-\frac{i\omega}{\gamma_e}\right)^2 - \frac{1}{1-G_{ei}L_{ei}}\left[G_{ee}L_{ee} + \frac{(G_{ese}L_{es}L_{se}+G_{esre}L_{es}L_{sr}L_{re})M_{es}M_{se}}{1-G_{srs}L_{sr}L_{rs}}\right], \qquad (17)$$

where $L_{ab}=(1-i\omega/\alpha_{ab})^{-1}(1-i\omega/\beta_{ab})^{-1}$, gain $G_{ab}=\rho_a\nu_{ab}$, and sigmoid slope $\rho_a=S'(V_a)$ is evaluated at the steady state. We define $G_{ese}=G_{es}G_{se}$, $G_{esre}=G_{es}G_{sr}G_{re}$, $G_{srs}=G_{sr}G_{rs}$, and $G_{esn}=G_{es}G_{sn}$ for convenience. Note that the dispersion relation for waves with wave number $k=0$ is given by $q^2(\omega)=0$; for more details, see [8,9,11]. Spectra and stability are linked by the fact that weak positive damping gives a strong spectral peak, and in the limit of zero damping the peak is infinite, while negative damping corresponds to instability. As in previous work [9,11,13,15], we set $\alpha_{ab}=\alpha$ and $\beta_{ab}=\beta$ for all ab, absorbing the effects of the many neurotransmitters into single effective rise and decay rates. Together with the parameters determining M_{es} and M_{se}, the power spectrum is described by nine parameters: α, β, γ_e, G_{ee}, G_{ei}, G_{ese}, G_{esre}, G_{srs}, and normalization $P_0=\langle\varphi_n^2\rangle G_{esn}/4\pi r_e^4 q^2(0)$. For single discrete delays $\tau_{es}=at_0$ and $\tau_{se}=(1-a)t_0$, $0\leqslant a\leqslant 1$ [16], $P(\omega)$ depends on just one extra parameter, the total corticothalamic loop delay t_0. Physiologically constrained parameters for the eyes-closed state are given in Table I.

TABLE I. Model parameters for the eyes-closed state, from [14], with the parameter a from [16]. CT=corticothalamic, TC=thalamocortical.

Quantity	Value	Unit	Description
γ_e	140	s^{-1}	Intracortical temporal damping rate
$1/\alpha$	13	ms	Decay time of cell body potential
$1/\beta$	3.5	ms	Rise time of cell body potential
t_0	84	ms	CT loop propagation time
a	0.25		TC fraction of total loop delay
G_{ee}	5.8		Excitatory intracortical gain
G_{ei}	−7.5		Inhibitory intracortical gain
G_{ese}	5.4		Gain for CT loop via relay nuclei
G_{esre}	−3.3		Gain for CT loop via reticular nucleus and relay nuclei
G_{srs}	−0.5		Gain for intrathalamic loop

Immediately from Eq. (16) we see that $P(\omega)$ is proportional to $|M_{es}(\omega)|^2$, but not to $|M_{se}(\omega)|^2$. This is because the drive ϕ_n into ϕ_s must propagate along connection es to reach the cortex; corticothalamic delays along connections se and re enter only via the $M_{es}M_{se}$ term in Eq. (17). Thus the power spectrum is acutely sensitive to the width of the thalamocortical delay distribution, with strong damping for $\omega\gtrsim 1/\sigma_{es}$ due to the $|M_{es}(\omega)|^2$ term in Eq. (16). For high power in the alpha band relative to lower frequencies, this cutoff must be above ~10 Hz, which requires $\sigma_{es}\lesssim 16$ ms.

III. RESULTS

We show the effects of distributed delays on the model power spectrum in Sec. III A, determine when it is appropri-

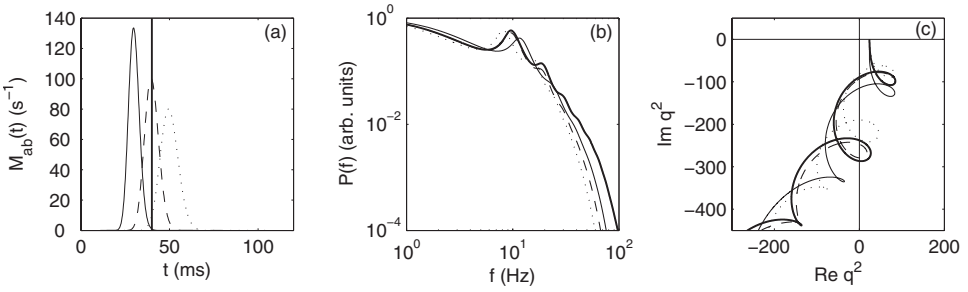

FIG. 2. Comparison of power spectra for discrete delay (thick line) and gamma-distributed delays with fixed relative widths $\sigma_{es}/\tau_{es}=\sigma_{se}/\tau_{se}=1/10$ for $\tau_{es}+\tau_{se}=60$ ms (solid), 80 ms (dashed), and 100 ms (dotted). (a) Delay distribution $M_{es}(t)=M_{se}(t)$. (b) Power spectrum $P(f)$. (c) $q^2(\omega)$; $q^2(0)$ lies on the real axis.

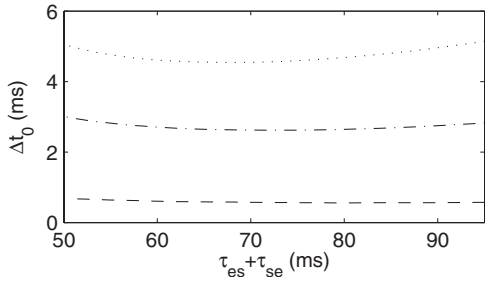

FIG. 3. Correction $\Delta t_0 = t_0 - (\tau_{es} + \tau_{se})$ to mean corticothalamic loop delay $\tau_{es} + \tau_{se}$ for a spectrum with discrete delay t_0 to have the same alpha frequency as for the distributed delays, for fixed $\sigma_{es}/\tau_{es} = \sigma_{se}/\tau_{se} = 1/10$ (dashed), 1/5 (dash-dotted), and 1/4 (dotted).

ate to replace a distribution with one or more discrete delays in Sec. III B, and determine when it is appropriate to replace a distributed delay with an ODE representation in Sec. III C.

A. Spectra with distributed delays

First we show that the alpha peak frequency depends on the sum of the mean delays $\tau_{ese} = \tau_{es} + \tau_{se}$ in the same way as it does on t_0 in the discrete case, apart from a small, width-dependent, correction. Figure 2 shows $P(\omega)$ and $q^2(\omega)$ for $M_{ab}(t)$ given by the gamma distribution (4) with $\tau_{es} = \tau_{se} = 30$, 40, and 50 ms, and with fixed relative widths $\sigma_{es}/\tau_{es} = \sigma_{se}/\tau_{se} = 1/10$. The case of fixed widths is similar. Other parameters are as given in Table I. Increasing τ_{ese} shifts the alpha peak to lower frequencies. The discrete delay $t_0 = \tau_{ese} + \Delta t_0$, where Δt_0 is a small correction, yields a power spectrum with the same alpha peak frequency as for the distribution. This quantity is plotted in Fig. 3 for relative widths $\sigma_{es}/\tau_{es} = \sigma_{se}/\tau_{se} = 1/10$, 1/5, and 1/4. For the parameters shown here, the effective t_0 is greater than the mean loop delay by less than 6 ms, and the correction increases with σ; for other parameters that give a sharper alpha peak, Δt is negative, but still increases in magnitude with σ. The behavior is similar when $M_{es}(t)$ and $M_{se}(t)$ are given by the truncated Gaussian distribution (6) with the same τ_{ab} and σ_{ab} as above, implying that it is the mean and width of the distribution that are important for the power spectrum at the alpha frequency, rather than the specific functional form $M_{ab}(t)$. This is in agreement with Eq. (12), in that the low-frequency behavior will agree for different distributions if the low-order moments agree, provided that differences in higher-order terms in Eq. (12) are comparatively small (which is satisfied for a wide range of distributions). This also implies that the sign of Δt does not simply reflect the distribution's skewness, which is negligible for Eq. (6) when $\sigma \ll \tau$.

Next we show how the power spectrum (16) changes with increasing thalamocortical delay width σ_{es}, holding the discrete corticothalamic delay constant (i.e., $\sigma_{se} = 0$). Figures 4(a)–4(c) show $P(\omega)$ and $q^2(\omega)$ for $M_{es}(t)$ given by the gamma distribution (4) with $\sigma_{es} = 0$, 4, 10, 20, and 40 ms. Mean thalamocortical and corticothalamic delays $\tau_{es} = \tau_{se} = 40$ ms are equal, giving corresponding $n_{es} = (\tau_{es}/\sigma_{es})^2 = \infty, 100, 16, 4, 1$, and thus each nonzero delay width shown admits an equivalent ODE of order n_{es}.

Increasing σ_{es} reduces power at high frequencies relative to the discrete delay case, due to the $|M_{es}|^2$ term in Eq. (16), as shown in the previous section. The cutoff moves to lower frequencies with increasing width, eliminating the alpha peak. As a secondary effect, the alpha peak power is reduced even for narrow distributions whose cutoff is well beyond the alpha band. This is due to the $M_{es}M_{se}$ term in Eq. (17). We show the effect of this by increasing σ_{se} with discrete thalamocortical delay fixed (i.e., $\sigma_{es} = 0$, eliminating the damping due to $|M_{es}|^2$). The resulting spectra are shown in Figs. 4(d)–4(f). All spectra match the discrete case at both low and high frequencies, while peaks in the alpha and beta bands are made less sharp by increasing σ_{se}. This is due to $q^2(\omega)$ tracing out smaller loops in the complex plane than it does in the discrete delay case, giving spectral peaks with lower Q-factors. Thus the system becomes more stable with increasing delay width, and less stable with decreasing delay width. This has also been demonstrated in the general setting

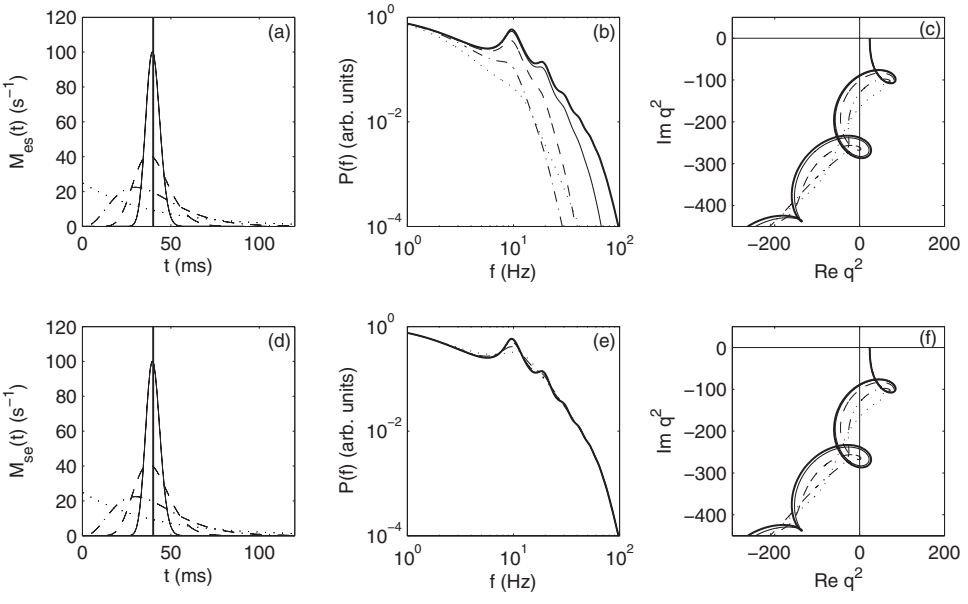

FIG. 4. Comparison of power spectra for discrete and gamma-distributed delays with fixed means $\tau_{es} = \tau_{se} = 40$ ms, changing thalamocortical (top row) and corticothalamic (bottom row) delay widths. (a) Delay distribution $M_{es}(t)$ for $\sigma_{es} = 0$ (thick vertical line), $\sigma_{es} = 4$ ms (solid), $\sigma_{es} = 10$ ms (dashed), $\sigma_{es} = 20$ ms (dash-dotted), and $\sigma_{es} = 40$ ms (dotted). (b) Power spectrum $P(f)$ for each $M_{es}(t)$ in (a), with $\sigma_{se} = 0$ in all cases. (c) $q^2(\omega)$; $q^2(0)$ lies on the real axis. (d) Same as (a) but for varying width of $M_{se}(t)$. (e) Power spectrum $P(f)$ for each $M_{se}(t)$ in (d), with $\sigma_{es} = 0$ in all cases. (f) Same as (c).

of coupled networks [7,18], and in a neural field model with delayed feedback [5] (although the authors did not explicitly state this). This result implies that when approximating a distribution of delays with a single discrete delay, other parameters must change in order to preserve the peak alpha power, or, in cases in which stability is lost, to retain even qualitatively similar solutions.

We now allow $\tau_{es} \neq \tau_{se}$ by setting $\tau_{es}=a\tau_{ese}$ and $\tau_{se}=(1-a)\tau_{ese}$, where $0 \leqslant a \leqslant 1$ is the thalamocortical fraction of the loop delay. The partitioning of the corticothalamic loop between the *es* and *se* connections has no effect on the spectrum for single discrete delays [16], since $|M_{es}|^2=1$ in Eq. (16) and $M_{es}M_{se}=1$ in Eq. (17). This is not true in general for distributed delays, but holds to a good approximation under mild conditions. Since the total mean delay $\tau_{es}+\tau_{se}$ is independent of the partitioning, any change to the alpha peak is due to the distribution widths. Holding relative widths constant and varying a, the alpha peak power and frequency only vary by at most a few percent provided that $\sigma_{es} \lesssim 16$ ms is satisfied. At high frequencies, $|M_{es}|^2 \sim \omega^{-2n_{es}}$ for $n_{es}=(a\tau_{ese}/\sigma_{es})^2$, so the slope of the spectrum will change with a at fixed σ_{es}, but this effect will typically be above the range of frequencies of interest in EEG. Thus the power spectrum depends only weakly on the delay partition, in good agreement with the discrete delay case.

B. Approximating distributions with a discrete delays

In this section, we show that distributed thalamocortical and corticothalamic delays are well approximated by discrete delays for the frequencies of interest in typical EEG studies, even for relatively wide distributions with widths 25% of their means, provided that other model parameters are moderately adjusted. Alternatively, adding a second discrete delay enables a good approximation without any parameter adjustment.

We showed in Sec. III A that the alpha peak frequency for a given delay distribution can be matched by using a discrete delay near the distribution mean, holding other model parameters constant. However, in this case the alpha peak power is significantly increased in moving to discrete delays, possibly to the extent that stability is lost. To counter this, we minimize the difference between the spectra by adjusting the other model parameters. The restriction to frequencies $\omega < \omega_m$ discussed in Sec. II A still applies, however, because the asymptotic slope of the spectrum is independent of all parameters besides those determining $M_{es}(\omega)$.

The optimal adjusted parameters are those that give the best least-squares fit of a spectrum with discrete delays to the spectrum with distributed delays, with the fitted range restricted to $\omega < \omega_m$. For illustrative purposes we use the parameters of Table I and Gaussian-distributed delays given by Eq. (6), fixing $\tau_{es}=\tau_{se}=40$ ms, and using relative widths 25% of these values. Figure 5 compares the spectra for Gaussian-distributed delays to the corresponding single discrete delay, with and without parameter adjustment. The adjusted parameters minimize $\Sigma_\omega\{\log[P_{\rm disc}(\omega)]-\log[P(\omega)]\}^2$, and are obtained using a Levenberg-Marquardt algorithm [24]. Using the log spectra gives roughly equal weight to

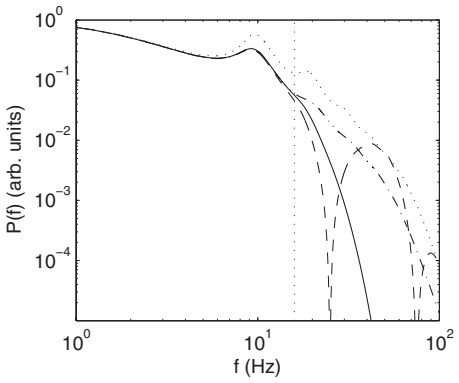

FIG. 5. Comparison of power spectra for Gaussian-distributed delays (solid), a single discrete delay (dotted), a single discrete delay with parameter adjustment (dash-dotted), and a pair of discrete delays (dashed). All cases have $\tau_{es}=\tau_{se}=40$ ms. The Gaussian and pair of discrete delays both have $\sigma_{es}=\sigma_{se}=10$ ms. The vertical dotted line denotes $f=\omega_m/2\pi=1/2\pi\sigma_{es}$.

spectral features in all frequency bands. Using a linear fit would underemphasize key physics at both high and low frequencies [9,13,14], the former due to there being relatively low power there, the latter due to there being relatively few points contributing to the fit. Parameters t_0, α, β, γ_e, G_{ee}, G_{ei}, G_{ese}, G_{esre}, and G_{srs} are allowed to vary, and spectra are normalized to have $P(0)=1$. Fits are restricted to 1 Hz $< f < 1/(2\pi\sigma_{es})$. The fitted spectrum differs from the actual spectrum by less than 2% over the fitted range. The bulk of the parameter adjustment is in the temporal parameters t_0, α, β, and γ_e, changing by −12%, −34%, +6%, and −23%, respectively, while the gains are adjusted by at most 3%. Note that the fitted t_0 is less than τ_{ese}, contrary to the result in Fig. 3, due to α and γ_e decreasing to fit the overall shape of the spectrum, whereas Δt_0 obtained earlier is the adjustment for only the alpha peak frequency.

Instead of adjusting parameters, the approximation is also improved by using a pair of discrete delays, the advantage being that two discrete delays together can have the same mean, width, and skewness as the Gaussian distribution. The restriction to $\omega \lesssim 1/\sigma_{es}$ is necessary here, to avoid the strong damping discussed in Sec. II A. The dash-dotted curve in Fig. 5 is the spectrum for two equally weighted delays ($c_1=c_2=1/2$) at $\tau_1=\tau_{es}-\sigma_{es}$ and $\tau_2=\tau_{es}+\sigma_{es}$ (and similarly for the *se* connection). This distribution has the same mean, width, and skewness as the Gaussian distribution above, i.e., the distributions agree to third order in Eq. (12). Note that for $\omega \lesssim 1/\sigma_{es}$, the pair of delays is superior to a single delay without parameter adjustment. The alpha peak power differs by <3% while its position differs by <1%, without needing to change any of the model parameters. Using three or more discrete delays improves the agreement further, as each additional delay enables matching of an additional two moments in Eq. (12), which also increases the upper limit on frequency.

In summary, for $f \lesssim 1/(2\pi\sigma_{es})$, a discrete delay is a good approximation to a distribution if other parameters are adjusted slightly. Alternatively, a pair of delays is also a good approximation, and does not require changing other parameters. Additional discrete delays are needed to approximate

spectra at higher frequencies. Parameter adjustment at different levels of modeling detail is consistent with the parameters in a mean-field model taking effective values averaging over the underlying physiology. Experimental values are themselves estimates of the true values, which are not known precisely anyway. Using a more realistic representation of the delays will likely yield better estimates of other parameters at the cost of more complexity.

C. Approximating distributions with ODEs

In this section, we show how narrow a distribution can be for it to still be approximated by a low-order ODE. The motivation for this is that gamma-distributed delays with integer n_{ab} allow an equivalent ODE representation, which, if of sufficiently low order, is more easily integrated than the convolution in Eq. (1) and has fewer storage requirements than if the distribution is approximated by a discrete delay, giving a DDE.

The question of whether an arbitrary distribution can be approximated by an ODE amounts to whether its transfer function is approximately of the form $M_{ab}(\omega)=R(i\omega)$, where $R(i\omega)$ is a rational function of $i\omega$. This is satisfied for any distribution that is well approximated by a gamma distribution of order n, where n is an integer. Since this wide class of distributions captures the main features of unimodal distributions with non-negative skewness, and since the model power spectrum at low frequencies is most sensitive to broad features of $M_{ab}(t)$ such as mean and width, an ODE approximation is sound if $M_{ab}(t)$ is well approximated by a gamma distribution. The problem then reduces to whether the order of the corresponding ODE is sufficiently low to be useful.

The order $n_{ab}=(\tau_{ab}/\sigma_{ab})^2$ grows rapidly with decreasing relative width, such that even for a relatively wide distribution with 25% relative width, the equivalent ODE is sixteenth order. If $n_{ab}^{\max}$ is the maximum order ODE desired, the distribution can be no wider than $\sigma_{ab}=\tau_{ab}/\sqrt{n_{ab}^{\max}}$. For thalamocortical delays, this maximum width imposes a maximum frequency cutoff at $\omega_m=\sqrt{n_{es}^{\max}}/\tau_{es}$. Thus a low-order ODE governing the thalamocortical delay will only yield sharp spectral peaks if σ_{es} (and thus τ_{es}) is small.

IV. SUMMARY AND DISCUSSION

In this paper, we have incorporated distributed delays into a mean-field corticothalamic model, and shown under what conditions a distribution can be replaced by one or more discrete delays, or by an equivalent ODE.

The main results are as follows. (a) A distribution of delays acts as a linear filter, and the distribution width σ constrains the frequencies transmitted to satisfy $\omega \lesssim \omega_m=1/\sigma$. Signals are heavily damped beyond this frequency. (b) Due to this damping, the model EEG power spectrum is sensitive to the width of the thalamocortical delay distribution. This asymmetry between the thalamocortical and corticothalamic pathways is because external drives must travel along the thalamocortical pathway to reach the cortex. (c) The alpha peak frequency depends on the sum of the mean thalamocortical and corticothalamic delays in the same way as it does on t_0 in the discrete case, apart from a small, width-dependent, correction. (d) A discrete delay is a good approximation to a distribution of delays if the other model parameters are adjusted slightly to compensate for taking an effective value. (e) Two discrete delays whose sum has the same mean, variance, and skewness as the distribution approximate the distribution without needing parameter adjustment. (f) Delay distributions with large fractional widths are well approximated by low-order ODEs.

The sensitivity of the power spectrum to the width of the thalamocortical delay distribution imposes a frequency cutoff at $\omega=1/\sigma_{es}$. This implies that a narrow distribution is needed for the thalamocortical pathway to prevent strong damping of the power spectrum at high frequencies. A narrow thalamocortical delay distribution has indeed been measured in the mouse [17]. The human delay distribution can be no wider than $\sim$16 ms to allow appreciable power in the alpha band relative to lower frequencies. Since the thalamocortical delay is likely to be a factor of 3 or more shorter than the corticothalamic delay [16], if $\tau_{es}\approx 20$ ms even a relatively wide fractional width of 25% is comfortably within this range.

Our results suggest that attentional focus could be aided by selecting a pathway with a narrower delay distribution, since this carries the system nearer to marginal stability, thereby increasing the strength of the response to stimuli. This is in agreement with a study on auditory evoked potentials [25], where the thalamocortical loop delay was found to be slightly but robustly shorter in response to target stimuli than background stimuli: if this corresponds to selection of a fast subset of the full distribution, the spread in delays is decreased. Furthermore, evoked potentials themselves are generated in the thalamocortical loop, with the peaks and troughs in the waveforms strongly dependent on the underlying conduction delays. How these waveforms change under distributed delays is a direction for future work.

Alternatively, involvement of a wider range of delays under varied sensory input acts to damp the system, insulating it from instability. This implies a possible route to seizure in the form of over-representation of a group of fibers with narrowly distributed delays. Such a mechanism is distinct from notions of excitation outweighing inhibition [15], relying instead on increased synchrony due to neuronal inputs arriving over narrower time windows.

ACKNOWLEDGMENT

The Australian Research Council supported this work.

[1] P. L. Nunez, *Neocortical Dynamics and Human EEG Rhythms* (Oxford University Press, New York, 1995).
[2] V. K. Jirsa and H. Haken, Phys. Rev. Lett. **77**, 960 (1996).
[3] S. Guo and L. Huang, Phys. Rev. E **67**, 011902 (2003).
[4] P. L. Nunez and R. Srinivasan, *Electrical Fields of the Brain* (Oxford University Press, New York, 2006).
[5] F. M. Atay and A. Hutt, SIAM J. Appl. Dyn. Syst. **5**, 670 (2006).
[6] A. Hutt and F. M. Atay, Phys. Rev. E **73**, 021906 (2006).
[7] T. Omi and S. Shinomoto, Phys. Rev. E **77**, 046214 (2008).
[8] P. A. Robinson, C. J. Rennie, and J. J. Wright, Phys. Rev. E **56**, 826 (1997).
[9] P. A. Robinson, C. J. Rennie, J. J. Wright, H. Bahramali, E. Gordon, and D. L. Rowe, Phys. Rev. E **63**, 021903 (2001).
[10] P. A. Robinson, Phys. Rev. E **72**, 011904 (2005).
[11] P. A. Robinson, C. J. Rennie, and D. L. Rowe, Phys. Rev. E **65**, 041924 (2002).
[12] P. A. Robinson, R. W. Whitehouse, and C. J. Rennie, Phys. Rev. E **68**, 021922 (2003).
[13] P. A. Robinson, C. J. Rennie, D. L. Rowe, and S. C. O'Connor, Hum. Brain Mapp **23**, 53 (2004).
[14] D. L. Rowe, P. A. Robinson, and C. J. Rennie, J. Theor. Biol. **231**, 413 (2004).
[15] M. Breakspear, J. A. Roberts, J. R. Terry, S. Rodrigues, N. Mahant, and P. A. Robinson, Cereb. Cortex **16**, 1296 (2006).
[16] J. A. Roberts and P. A. Robinson, J. Theor. Biol. **253**, 189 (2008).
[17] M. Salami, C. Itami, T. Tsumoto, and F. Kimura, Proc. Natl. Acad. Sci. U.S.A. **100**, 6174 (2003).
[18] V. K. Jirsa and M. Ding, Phys. Rev. Lett. **93**, 070602 (2004).
[19] J. D. Murray, *Mathematical Biology*, 2nd ed. (Springer, Berlin, 1993).
[20] M. K. Stephen Yeung and S. H. Strogatz, Phys. Rev. Lett. **82**, 648 (1999).
[21] L. G. Nowak and J. Bullier, in *Cerebral Cortex*, edited by K. S. Rockland, J. H. Kaas, and A. Peters (Plenum, New York, 1997), Vol. 12, pp. 205–241.
[22] P. Girard, J. M. Hupé, and J. Bullier, J. Neurophysiol. **85**, 1328 (2001).
[23] *Handbook of Mathematical Functions*, edited by M. Abramowitz and I. A. Stegun (Dover, New York, 1965).
[24] W. H. Press, S. A. Teukolsky, W. T. Vetterling, and B. P. Flannery, *Numerical recipes in C*, 2nd ed. (Cambridge University Press, Cambridge, 1992).
[25] C. C. Kerr, C. J. Rennie, and P. A. Robinson, Biol. Cybern. **98**, 171 (2008).